In presenting the dissertation as a partial fulfillment of the requirements for an advanced degree from the Georgia Institute of Technology, I agree that the Library of the Institute shall make it available for inspection and circulation in accordance with its regulations governing materials of this type. I agree that permission to copy from, or to publish from, this dissertation may be granted by the professor under whose direction it was written, or, in his absence, by the Dean of the Graduate Division when such copying or publication is solely for scholarly purposes and does not involve potential financial gain. It is understood that any copying from, or publication of, this dissertation which involves potential financial gain will not be allowed without written permission.

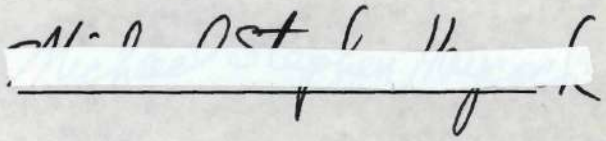

3/17/65
b

A COMPARISON OF TWO PROJECTILE CONFIGURATIONS FOR IMPACT TESTING

A Thesis

Presented to

The Faculty of the Graduate Division

by

Michael Stephen Haycock

In Partial Fulfillment

of the Requirements for the Degree

Master of Science in Engineering Mechanics

Georgia Institute of Technology

June, 1966

A COMPARISON OF TWO PROJECTILE CONFIGURATIONS

FOR IMPACT TESTING

Approved:

Chairman.

Date Approved by Chairman: 5/6/66

ACKNOWLEDGMENTS

I wish to thank Dr. C. E. Stoneking, my advisor, for his guidance in directing my energies. I also wish to thank Steve Passman, my friend, for his advice, counsel, and time spent helping me.

TABLE OF CONTENTS

	Page
ACKNOWLEDGMENTS	ii
LIST OF TABLES	iv
LIST OF ILLUSTRATIONS	v
SUMMARY	vi
Chapter	
I. INTRODUCTION	1
II. INSTRUMENTATION AND EQUIPMENT	3
III. DISCUSSION OF RESULTS	6
IV. CONCLUSIONS	9
V. RECOMMENDATIONS	10
APPENDIX	11
BIBLIOGRAPHY	40

LIST OF TABLES

Page

Table

1. Projectile Sizes. 13

2. Data for U1 14

3. Data for S1 16

4. Data for U2 17

LIST OF ILLUSTRATIONS

Page

Figure

1. Equipment Layout. 18
2. Firing Apparatus. 19
3. Projectile Holding Device 20
4. Velocity Measuring Apparatus. 21
5. Projectile Configuration. 22
6. Oscilloscope Triggering System. 23
7. An Example of a Faulty Electron Beam Weld 24
8. A Typical Projectile of Each Type After Impact. 25
9. A Typical Projectile of Each Type After Impact Well Above Failure Velocity. 26
10. Impact Area Diameter Versus Impact Velocity for U1. 27
11. Impact Area Diameter Versus Impact Velocity for S1. 28
12. Change in Axial Length Versus Impact Velocity for U1. 29
13. Change in Axial Length Versus Impact Velocity for S1. 30
14. Peak Impact Force Versus Impact Velocity for U1 31
15. Peak Impact Force Versus Impact Velocity for S1 32
16. Peak Impact Force Versus Change in Axial Length for U1. . . . 33
17. Peak Impact Force Versus Change in Axial Length for S1. . . . 34
18. Impact Area Diameter Versus Impact Velocity for U2. 35
19. Change in Axial Length Versus Impact Velocity for U2. 36
20. Peak Impact Force Versus Impact Velocity for U2 37
21. Peak Impact Force Versus Change in Axial Length for U2. . . . 38
22. A Typical Strain Gage Pulse 39

SUMMARY

A comparison was made under impact testing conditions between two projectile configurations. The object of the study was to investigate the possibility of replacing a hollow sphere with a test tube shape container for impact studies.

The phenomena compared were the following:

(1) failure velocity
(2) mode of failure
(3) peak impact force
(4) impact duration
(5) diameter of impacted surface
(6) change in axial length

Failure of a specimen was defined as the appearance of a crack on its outside surface.

The results were positive and indicated that the proposed replacement was feasible.

CHAPTER I

INTRODUCTION

The problem studied in this thesis has grown out of the Impact Effects Program (1), at the Georgia Institute of Technology, sponsored by Sandia Corporation, Albuquerque, New Mexico. In trying to obtain hollow spherical shells as specimens for impact testing, it was found that such a geometry is difficult to achieve within reasonable tolerances and cost limits. The most widely used means of achieving this geometry has been welding of two hemispheres. Since two pieces are machined to make each projectile, this method is both expensive and time-consuming. These pieces are welded together by either a Heliarc or Electron Beam process. Not only is this welding costly, but it involves the possibility of rupture around the weld. The effect of a bad weld is shown in Figure 7.

The purpose of this research was to investigate the possibility of replacing, for experimental use, the costly hollow spherical shell with a projectile which was less expensive and more easily manufactured. The shape used to simulate the hollow spherical specimen was one with a spherical nose and a cylindrical tail portion. The two different projectile shapes were compared in their responses to impact into a rigid target in the velocity range 250-450 fps. Specifically, the phenomena to be compared were the following:

(1) failure velocity
(2) mode of failure
(3) peak impact force

(4) impact duration
(5) diameter of impacted surface
(6) change in axial length

Failure of a specimen was defined as the appearance of a crack on its outside surface.

Although there have been many impact testing programs carried out by others (2,3) this researcher found no program related closely enough to this one to provide a comparison of the results obtained.

CHAPTER II

INSTRUMENTATION AND EQUIPMENT

The apparatus used in this experiment consisted of an air gun for firing the projectiles, a system for measuring projectile velocity, a Hopkinson Pressure Bar, and a system of strain gages. The general layout of the equipment is shown schematically in Figure 1.

The air gun was designed to operate with compressed air at a maximum pressure of 1500 psi. Operation of the gun involved storing a charge of pressure and releasing it rapidly. An air-operated piston was used to accomplish the rapid release of the stored charge; air for the operation of the piston was controlled by solenoid valves connected to the electronic triggering device as shown in Figure 2.

The projectile was held in place by a restraining pin attached to the barrel of the gun. This device, shown in Figure 3, restrained the projectile until the full charge pressure was acting on the projectile, thus yielding optimum efficiency from the gun.

Velocities of the projectiles were calculated by measuring the time interval required for a projectile to pass between two light beams spaced one foot apart. The disturbance of each light beam was detected by a separate photocell and relayed to a Beckman 6350 AWRU scaler. Both light sources were mounted on the barrel of the gun, as depicted in Figure 4.

The Hopkinson Pressure Bar (4) was made of die steel, hardened to Rockwell C60 to prevent plastic deformation. The bar, which was

supported in two places from the ceiling of the laboratory, measured $1\frac{1}{2}$ inches in diameter by 10 feet in length. This particular bar was made to these specifications by the Latrobe Steel Company, Latrobe, Pennsylvania.

Strain in the pressure bar was measured by BLH SR-4 type C7 strain gages. BLH switching and balancing units were used; the resulting signal was displayed on an HP 140A oscilloscope and recorded with a Polaroid oscilloscope camera. The trace of the oscilloscope was triggered by the pulse emitted from the last photocell which the projectile passed.

Projectiles of two types were used--the original hollow spherical shape, and the test tube shape that was designed to simulate its properties. These are exhibited in Figures 5 and 8. The dimensions for the hollow spheres used were chosen to agree with those used by the Impact Effects Program, and these are listed in Table 1. The diameter and wall thickness of the test tube shape were chosen to agree with those of the spheres. Thus the nose of the test tube shape was identical to the portion of a spherical projectile which was to be impacted. The cylindrical tail portion was designed to have a mass equal to that of the nose, giving a total mass equal to that of a hollow sphere with the same thickness and diameter. Thus, the kinetic energies of two projectiles of the same size but of the two different shapes were the same for identical impact velocities.

The required machining was done with a ball end mill and a radius tool of appropriate size. The hemispheres for the spherical projectiles were welded by a Tungsten Heliarc process using a fused

pass with no wire and a filler pass with type A-613 .030" wire. The bead from the weld was then removed, and the projectiles were hardened to Rockwell C40.

CHAPTER III

DISCUSSION OF RESULTS

The results, as expected, were positive and supported the suggested substitution of the U shape for the S shape for impact purposes. The bulk of the comparisons was made between size S1 and size U1, both of which had the same weight, diameter, and wall thickness. The third size, U2, did not yield any startling discrepancies when compared to size U1.

The mode of failure for U1 and S1 was the same. Both failed on the flat circular impacted surface in a circle concentric to that surface as shown in Figure 9. The failure velocity for S1 was in the range 300-310 fps, while the failure velocity for U1 was in the range 295-305 fps. It was not unreasonable, therefore, to consider the failure velocities of these two shapes as being the same. The behavior of the two shapes was practically the same for impacts at velocities up to 600 fps.

The duration of the impact was found to be approximately 50 microseconds for both shapes. This parameter was found to be independent of the impact velocity. Error in this measurement was ± 20% as shown in the Appendix.

The diameter of the flattened impact surface of the shape U1 was plotted against impact velocity in Figure 10. If one considered only the range of velocities 250-575 fps, the configuration of points was approximated by a straight line with a slope of 0.05 inches/fps. This line,

when extrapolated, had an intercept on the vertical axis of 0.240 inches at zero velocity. Since the origin had to be included as part of the graph, a positive intercept such as the one above indicated that the graph would not have been a straight line in the velocity range 0-250 fps.

The graph of the same parameter for the shape S1 was also linear for the range of 250-450 fps. Its slope was 0.055 inches/fps, and its intercept on the vertical axis was 0.200 inches, indicating good correlation between the responses of the two shapes.

Change in axial length versus impact velocity was plotted for shapes U1 and S1. The graphs for both shapes were considered as straight lines with slopes of 290 μ inches/fps and 310 μ inches/fps, respectively. The graphs first intersect the velocity axis at velocities of 50 fps and 40 fps, respectively. This indicated that there was no appreciable change in length until the impact velocity reached 40-50 fps. These graphs were in close agreement throughout the range of velocities tested.

Peak impact force was calculated by a static analysis of the strain in the pressure bar. Sample calculations of this operation are shown in the Appendix. Scatter in this data was evident; this was partly due to experimental error in the measurement of the pulse from the strain gage. The scatter was not broad enough, however, to cause serious doubts as to the validity of the readings.

Impact force was plotted against change in length in Figures 16 and 17. Linearity was assumed for the approximating curves, since no more preferable configuration was suggested by the data. The slopes for the graphs for shapes U1 and S1 were 2.3×10^5 lbs/inch and 2.4×10^5 lbs/inch,

respectively. Both extrapolated intercepts occurred on the force axis at approximately zero change in length. This indicated that there was no significant force registered before a change in length occurred.

The curves for static force versus impact velocity were assumed to be straight lines. Again, there was good agreement between the data for shapes S1 and U1. Both the extrapolated intercepts and the slopes were practically the same.

Data for the shape U2 were plotted similarly to those for shapes U1 and S1. Graphs of the U2 data were assumed to be linear and were found to have the same characteristics as the corresponding graphs for shapes S1 and U1.

In all three cases the curves representing the change in axial length and the diameter of the impact surface versus impact velocity appeared to flatten out at velocities above the range which was being investigated. However, this conclusion was not fully substantiated because of a lack of data in the high velocity region. The apparent tendency, however, did not conflict with any logical consideration of the phenomena. There most probably was a limiting diameter, and most certainly there was a limiting change in axial length associated with the impact of these shapes.

CHAPTER IV

CONCLUSIONS

It is concluded from the results of this experiment, that the shape U1 can be used in the place of shape S1 for the purpose of determining a failure velocity.

The duration of an impact is independent of the impacting velocity.

The mode of failure is the same for the shapes tested.

All characteristics of the two shapes which were measured are similar in nature and comparable in magnitude.

The number of test shots made was sufficient to insure the validity of the data because of the relatively small amount of scatter present in the data.

There was no discrepancy in the comparison, other than experimental error. This would indicate that the shape U1 could replace the shape S1 for experimental impact testing.

CHAPTER V

RECOMMENDATIONS

It is recommended that a similar testing program be executed for other sizes of the S shape and the U shape. This testing should be made over a larger scale of velocities and should therefore include more test specimens. The scatter of the data should be small enough so that a statistical approach might indicate small variations in the behaviour which are now obscured. The recommended testing program should include a variation in the hardness of the projectiles. The bulk of the testing may be done with the U shape, while the S shape may be used as a check for the results. The temperature should be held constant unless it is specifically desired as a variable. If positive test results from the above described investigation are obtained, it is recommended that the U shape be used exclusively in similar test programs in the future.

It is further recommended that a theoretical study of the stress distribution in a spherical shell under impact loading be carried on concurrently with an investigation as described above.

APPENDIX

The peak impact force was calculated from the strain gage readings with a one dimensional static analysis of the strain in the pressure bar. From the definition of gage factor;

$$G.F. = \frac{\Delta R}{R\epsilon}$$

a calibration strain was calculated with a calibration resistance of 1691 ohms. The strain gage resistance was 505 ohms. The calibration deflection was 0.15 volts and the corresponding calibration strain was 0.068 inches per inch. Since two strain gages were mounted on the pressure bar to eliminate a bending effect, the experimental strain was calculated from

$$\epsilon_{EXP} = \left(\frac{0.068}{0.15}\right) \frac{\delta_{EXP}}{2}$$

The one dimensional stress-strain relation

$$\sigma_{EXP} = E\ \epsilon_{EXP}$$

coupled with

$$\sigma = \frac{F}{A}$$

yielded

$$F = AE\ \epsilon_{EXP}$$

or

$$\text{Force} = (\pi)\ (\tfrac{3}{4})^2\ (30 \times 10^6)\ (\tfrac{.068}{.15})\ (\tfrac{1}{2})\ \delta_{EXP}$$

which may be written as

$$F = 13{,}250\ (\delta_{EXP})$$

where δ_{EXP} is the deflection reading from the oscilloscope trace in millivolts.

The duration of the impact was measured directly from the oscilloscope trace. It was the width in time units of the first pulse registered.

Error involved in this measurement was calculated by considering the true reading to be halfway between the reading obtained by measuring the distance between the outside edges of the pulse and the reading obtained by measuring the distance between the inside edges of the pulse. Figure 22 shows a typical pulse which indicates the error to be ± 20%.

Table 1

Projectile Sizes

Size	U1	U2	S1
O.D.	1.000"	1.000"	1.000"
Wall thickness	0.100"	0.130"	0.100"
Length	0.952"	0.939"	1.000"

Table 2

Data for U1

Shot No.	Velocity (fps)	Failure	Flat Diameter in. x 10^3	ΔL in. x 10^3	Peak (mv)	Force (kip)	Duration (msec)
1	680	yes	850	180	3.30	43.7	.05
2	568	yes	803	154	2.85	37.8	.05
3	562	yes	796	152	2.80	37.1	.05
4	558	yes	781	153	3.00	39.8	.05
5	550	yes	781	142	2.95	39.1	.05
6	538	yes	772	142	3.00	39.8	.05
7	529	yes	758	142	2.95	39.1	.05
8	521	yes	750	140	2.65	35.1	.05
9	515	yes	750	133	2.70	35.8	.05
10	513	yes	750	133	2.65	35.1	.05
11	510	yes	740	133	2.80	37.1	.05
12	507	yes	734	125	2.60	34.5	.05
13	486	yes	710	125	2.65	35.1	.05
14	478	yes	718	125	2.45	32.5	.05
15	453	yes	734	114	2.30	30.5	.05
16	437	yes	703	114	2.20	29.2	.05
17	418	yes	671	108	2.10	27.8	.05
18	376	yes	625	92	2.25	29.8	.05
19	351	yes	593	84	--	--	.05
20	318	yes	550	77	1.80	23.9	.05
21	314	yes	546	84	1.80	23.9	.05
22	308	yes	546	70	1.70	22.5	.05
23	302	no	530	77	1.60	21.2	.05

(Continued)

Table 2 (Concluded)

Shot No.	Velocity (fps)	Failure	Flat Diameter in. x 10^3	ΔL in. x 10^3	Peak (mv)	Force (kip)	Duration (msec)
24	298	no	528	70	1.70	22.5	.05
25	298	no	540	70	1.70	22.5	.05
26	298	yes	531	69	1.80	23.9	.05
27	291	no	512	70	1.60	21.2	.05
28	289	no	515	70	--	--	.05
29	284	no	518	70	1.45	19.2	.05
30	276	no	531	62	--	--	.05
31	275	no	468	62	--	--	.05
32	270	no	493	69	1.65	21.9	.05
33	268	no	500	62	--	--	.05
34	266	no	500	55	--	--	.05
35	174	no	375	31	1.70	22.5	.05

Table 3

Data For S1

Shot No.	Velocity (fps)	Failure	Flat Diameter in. x 10^3	ΔL in. x 10^3	Peak (mv)	Force (kip)	Duration (msec)
1	720	yes	906	190	3.70	99.0	.05
2	654	yes	750	147	3.10	41.1	.05
3	454	yes	703	125	2.50	33.1	.05
4	440	yes	686	125	2.40	31.8	.05
5	434	yes	656	118	2.75	36.4	.05
6	424	yes	671	125	2.40	31.8	.05
7	413	yes	656	110	2.25	29.8	.05
8	392	yes	632	107	2.00	22.5	.05
9	373	yes	617	103	2.05	27.2	.05
10	358	yes	585	94	2.00	26.5	.05
11	340	yes	578	94	2.10	27.8	.05
12	311	yes	550	85	--	--	.05
13	311	no	522	75	--	--	.05
14	310	no	528	79	1.85	29.5	.05
15	305	yes	512	79	1.90	25.2	.05
16	302	yes	515	70	2.20	29.2	.05
17	302	yes	525	77	2.40	31.8	.05
18	290	no	508	79	1.60	21.2	.05
19	278	no	506	79	1.65	21.9	.05
20	236	no	350	54	1.10	14.6	.05

Table 4

Data for U2

Shot No.	Velocity (fps)	Failure	Flat Diameter in. x 10^3	ΔL in. x 10^3	Peak (mv)	Force (kip)	Duration (msec)
1	685	yes	812	150	3.45	45.7	.05
2	628	yes	796	162	4.10	54.3	.05
3	617	yes	656	104	4.40	58.3	.05
4	613	yes	819	151	--	--	.05
5	595	yes	796	143	--	--	.05
6	568	yes	790	143	3.75	49.7	.05
7	474	yes	703	110	3.25	43.1	.05
8	429	yes	671	96	3.10	41.1	.05
9	382	yes	617	87	2.75	36.4	.05
10	350	yes	578	79	2.65	35.1	.05
11	325	yes	553	71	2.45	32.5	.05
12	307	yes	531	64	2.30	30.5	.05
13	292	yes	515	57	2.30	30.5	.05
14	270	no	484	56	2.20	29.2	.05
15	262	yes	475	49	2.00	26.5	.05
16	240	yes	444	49	1.80	23.9	.05
17	228	yes	444	49	1.70	22.5	.05
18	222	no	406	41	1.85	24.5	.05
19	208	no	406	41	1.65	21.9	.05

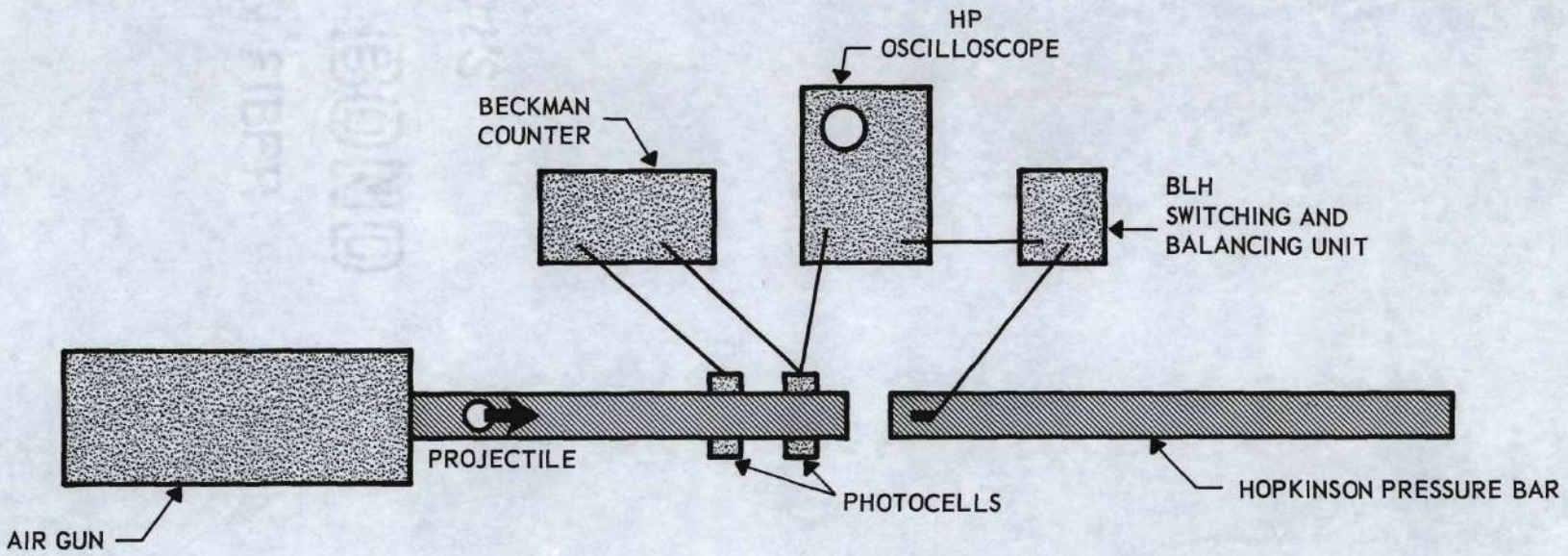

Figure 1. Equipment Layout.

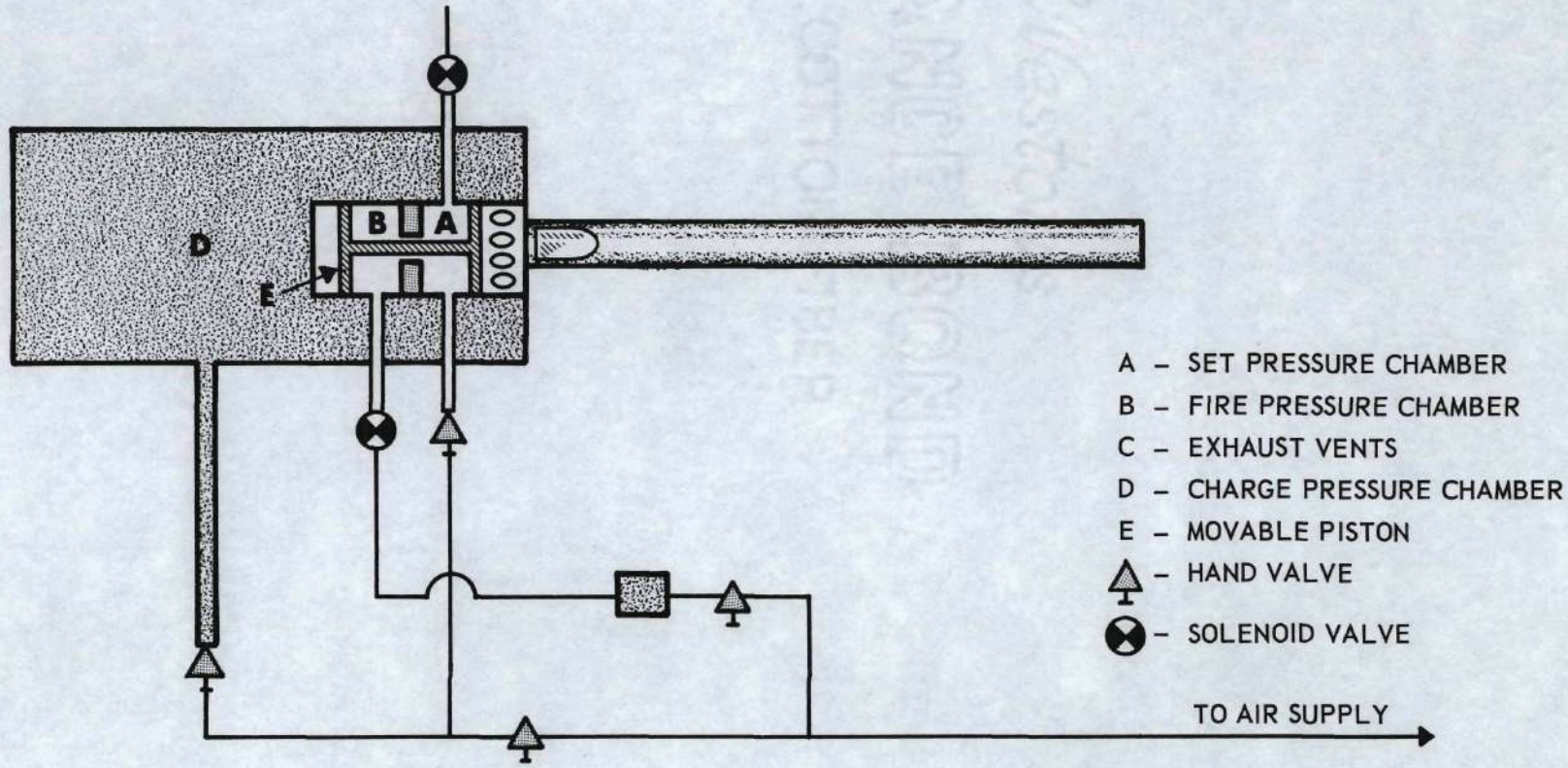

Figure 2. Firing Apparatus.

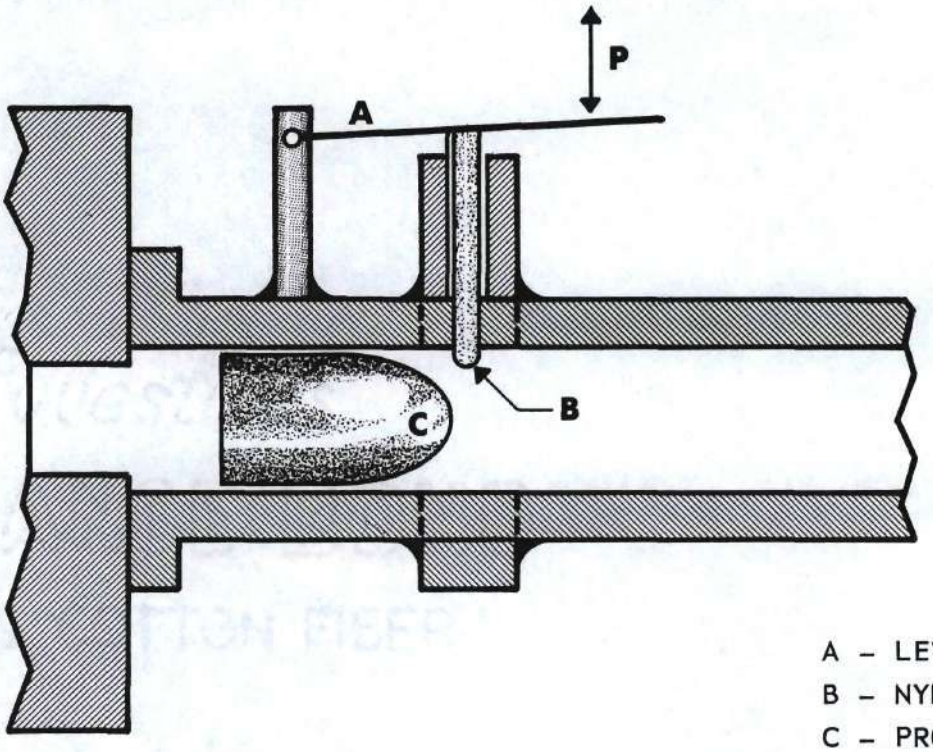

A – LEVER
B – NYLON PIN
C – PROJECTILE
P – VARIABLE FORCE

Figure 3. Projectile Holding Device.

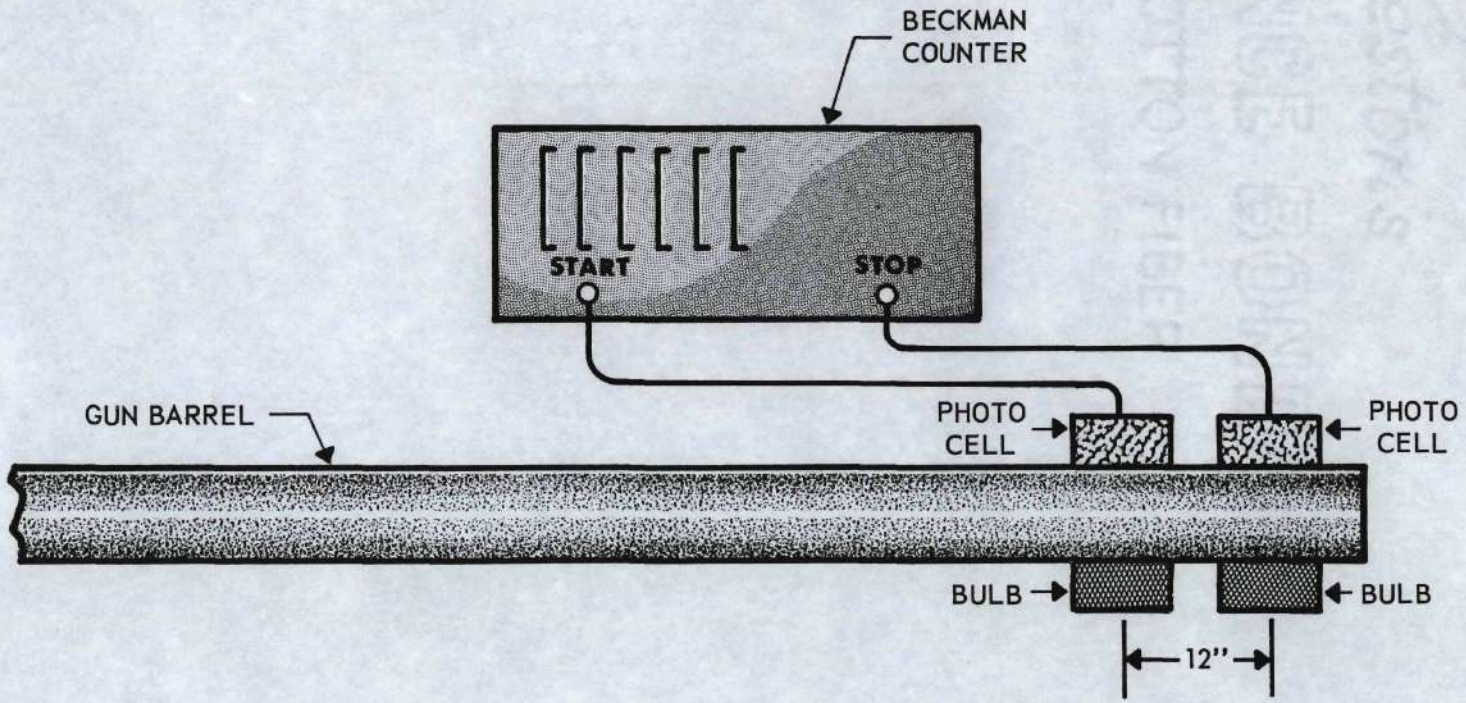

Figure 4. Velocity Measuring Apparatus.

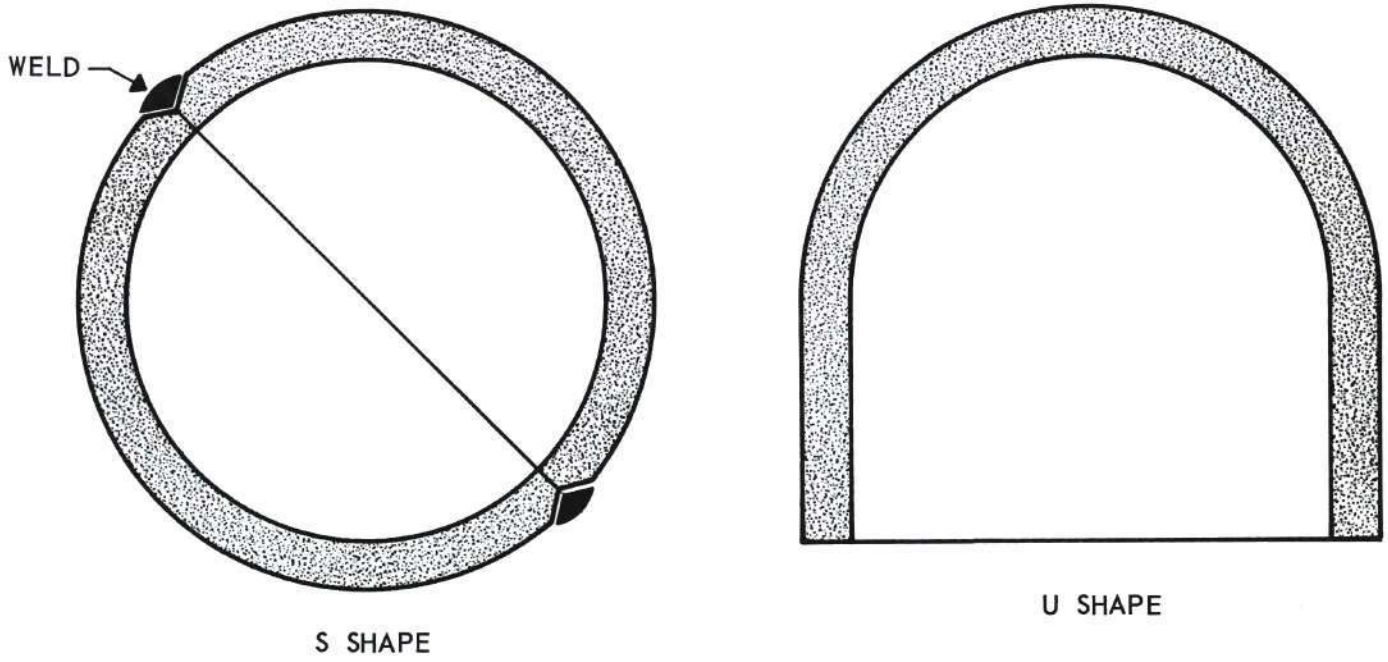

Figure 5. Projectile Configuration.

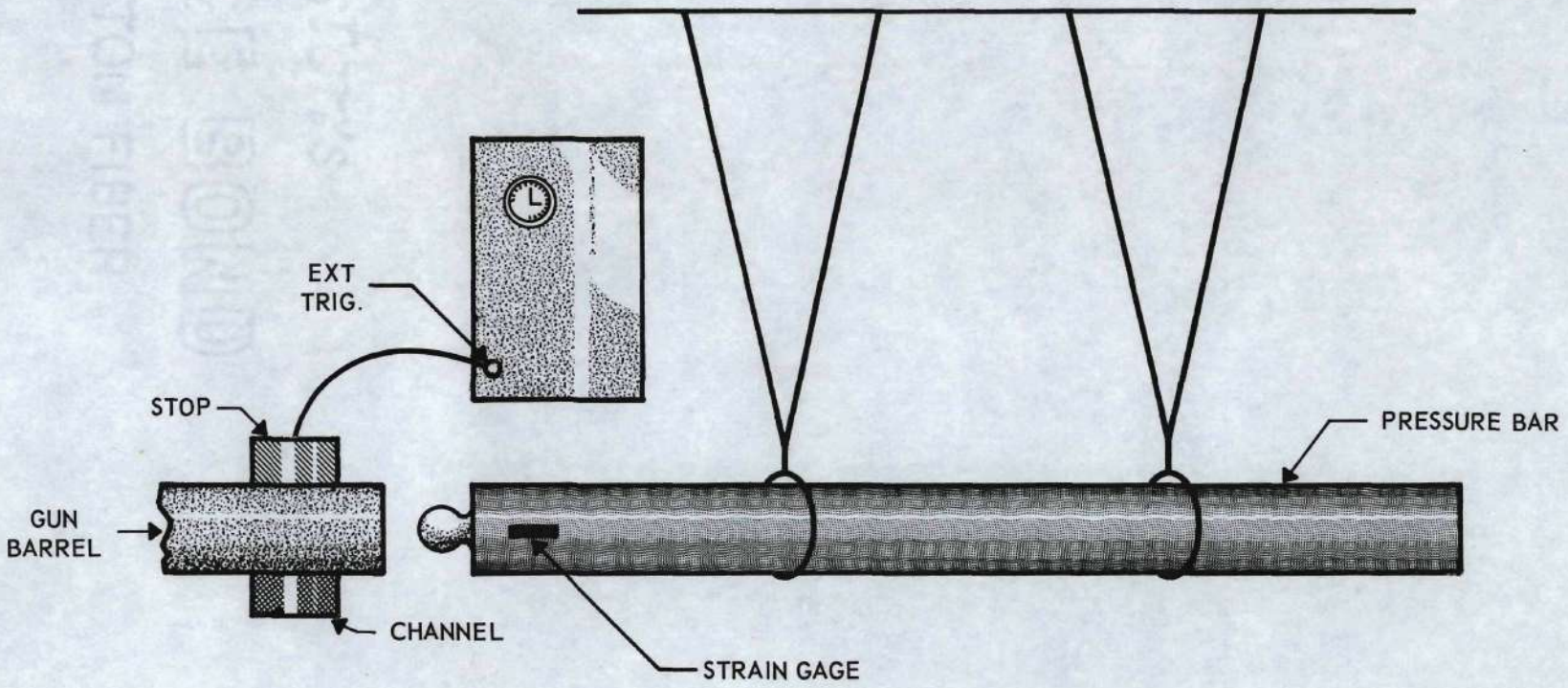

Figure 6. Oscilloscope Triggering System.

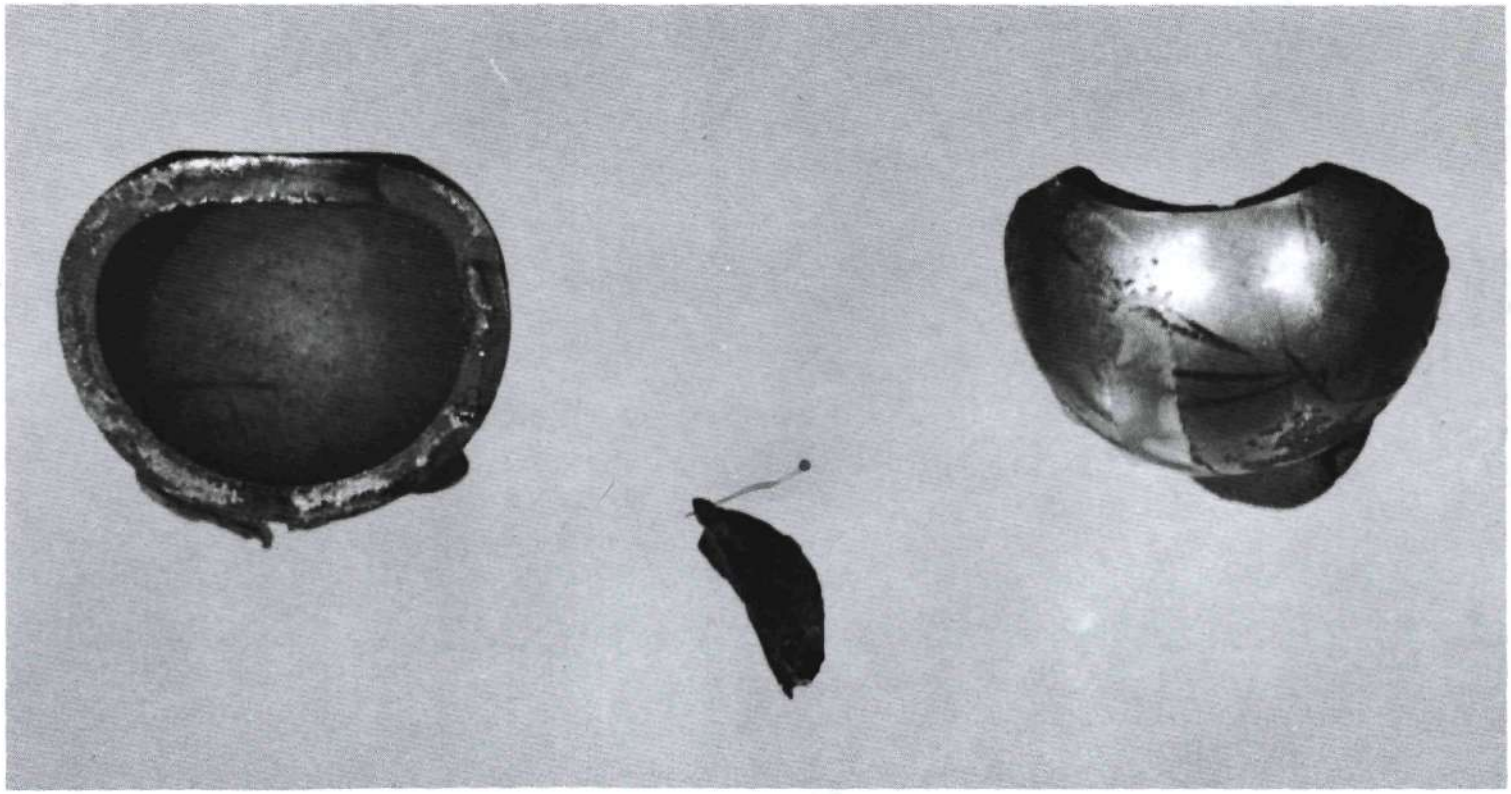

398 fps

Figure 7. An Example of a Faulty Electron Beam Weld.

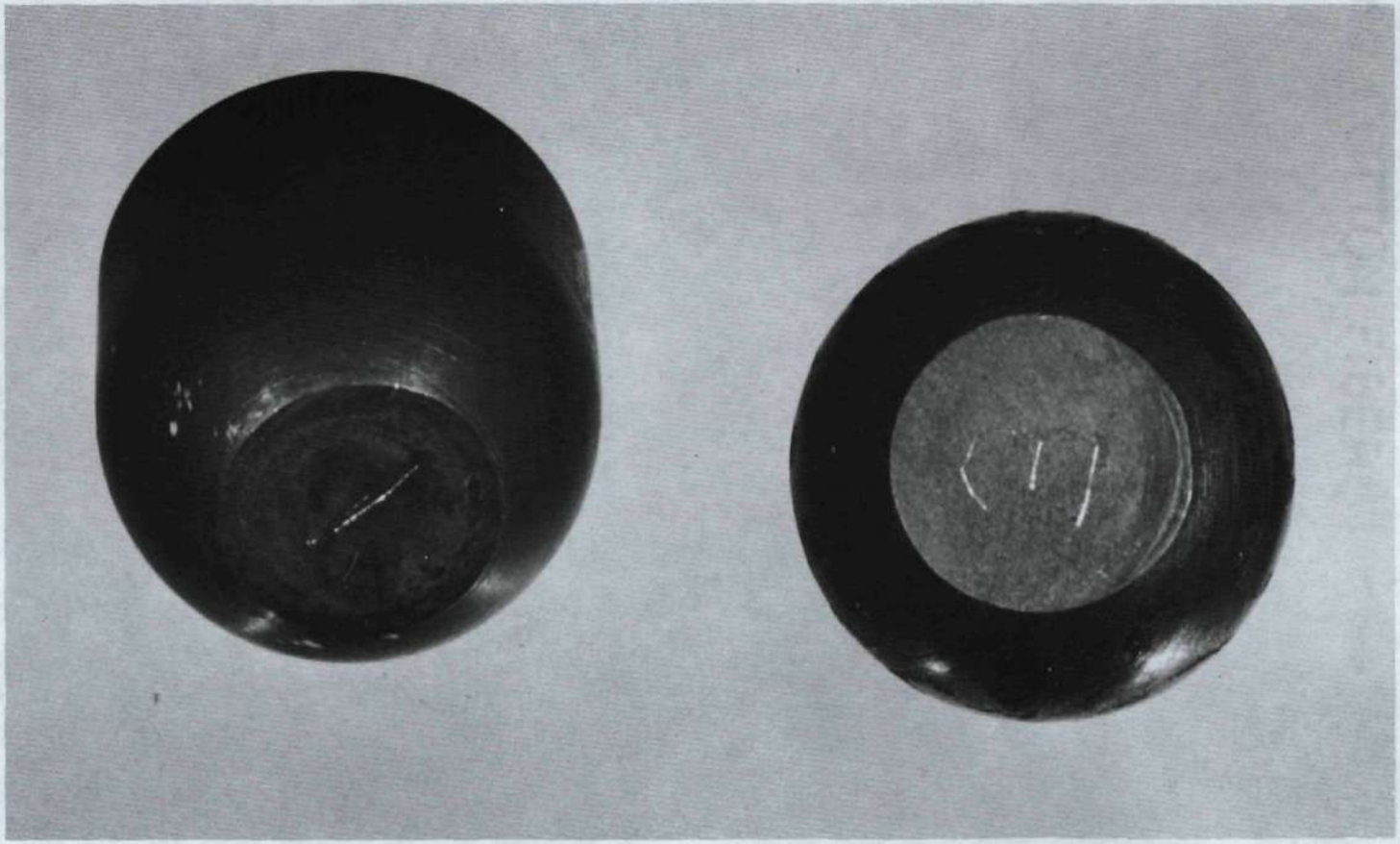

298 fps 340 fps

Figure 8. A Typical Projectile of Each Type After Impact.

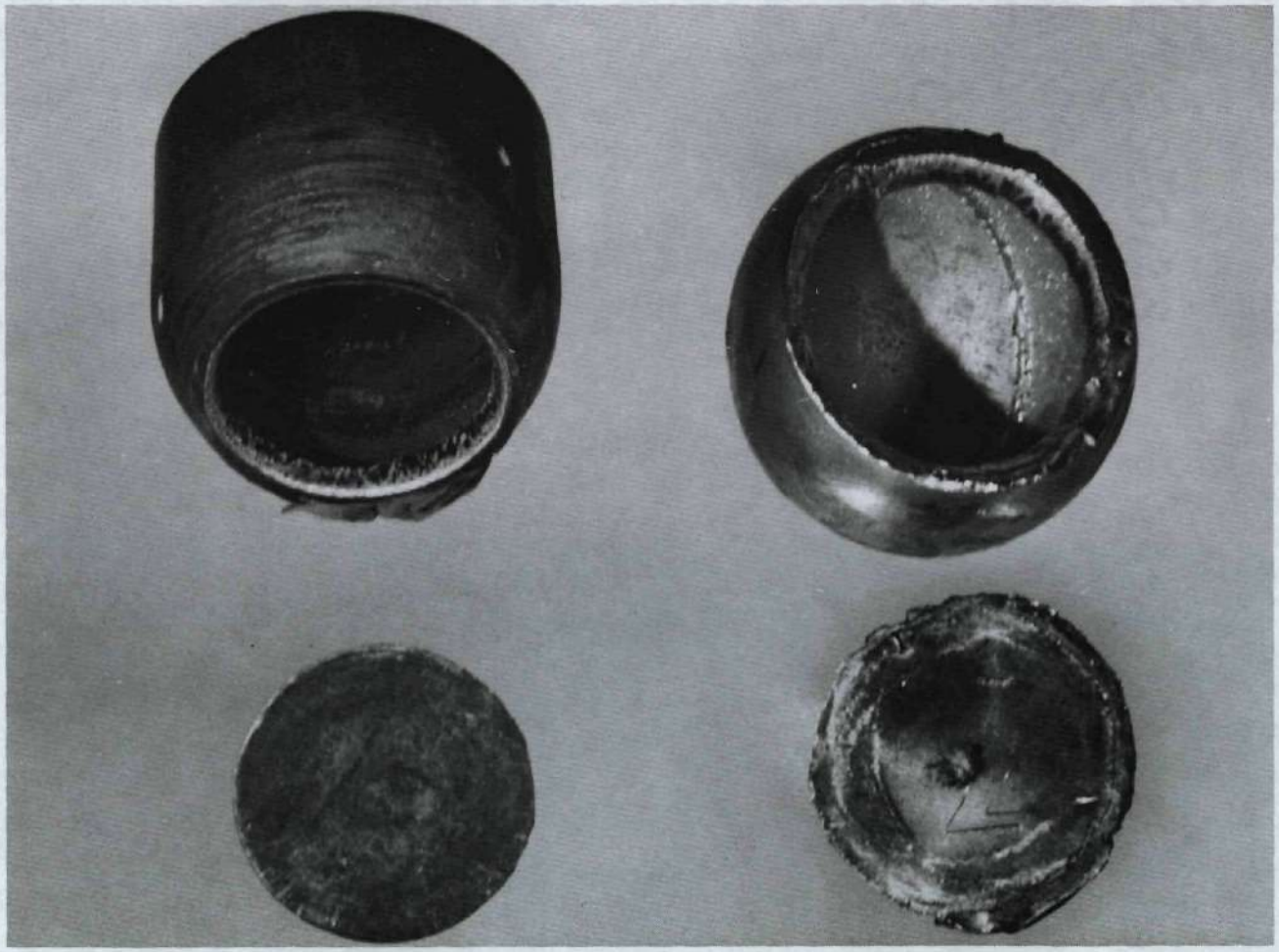

562 fps

720 fps

Figure 9. A Typical Projectile of Each Type After Impact Well Above Failure Velocity.

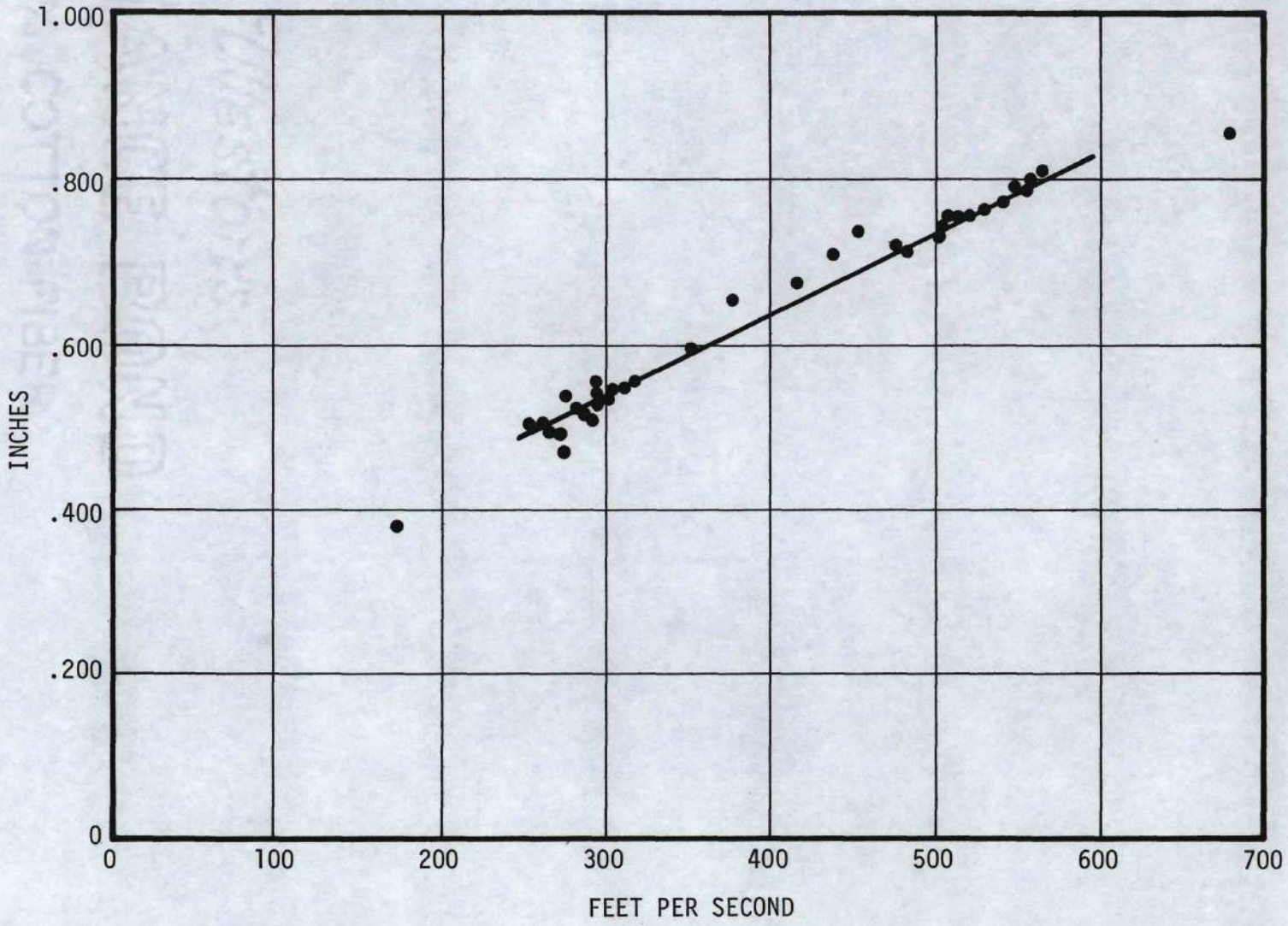

Figure 10. Impact Area Diameter Versus Impact Velocity of U1.

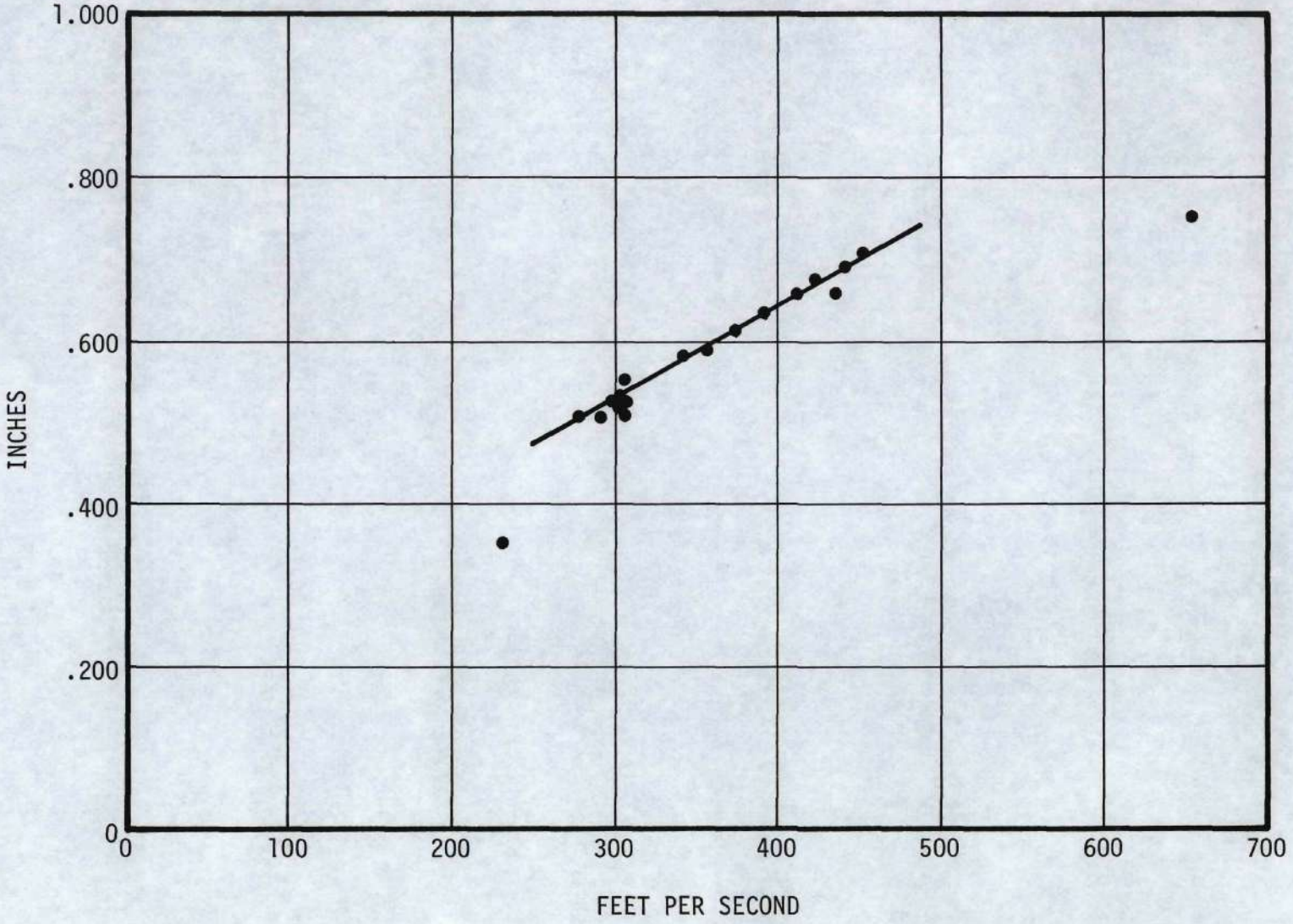

Figure 11. Impact Area Diameter Versus Impact Velocity for S1.

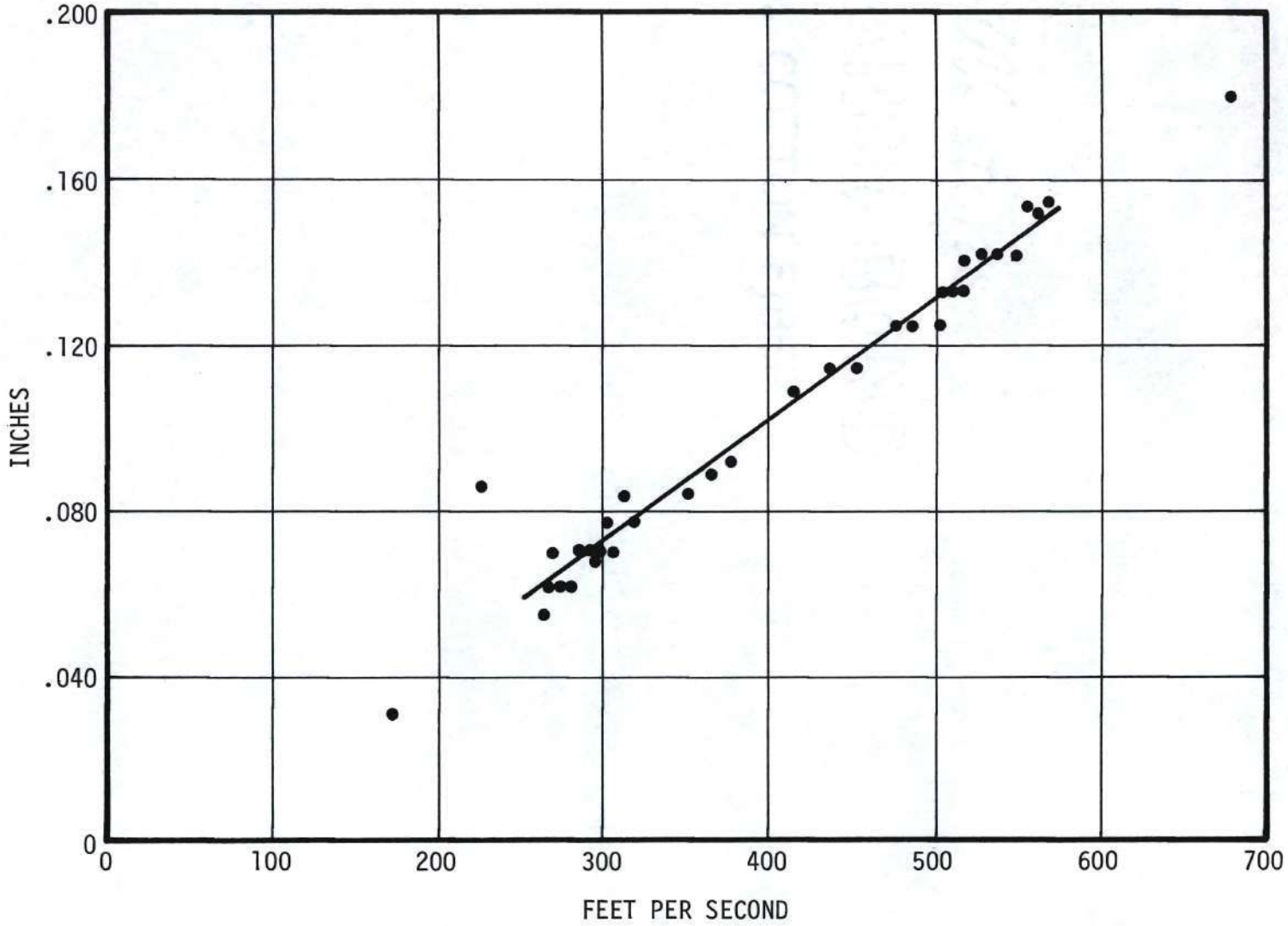

Figure 12. Change in Axial Length Versus Impact Velocity for U1.

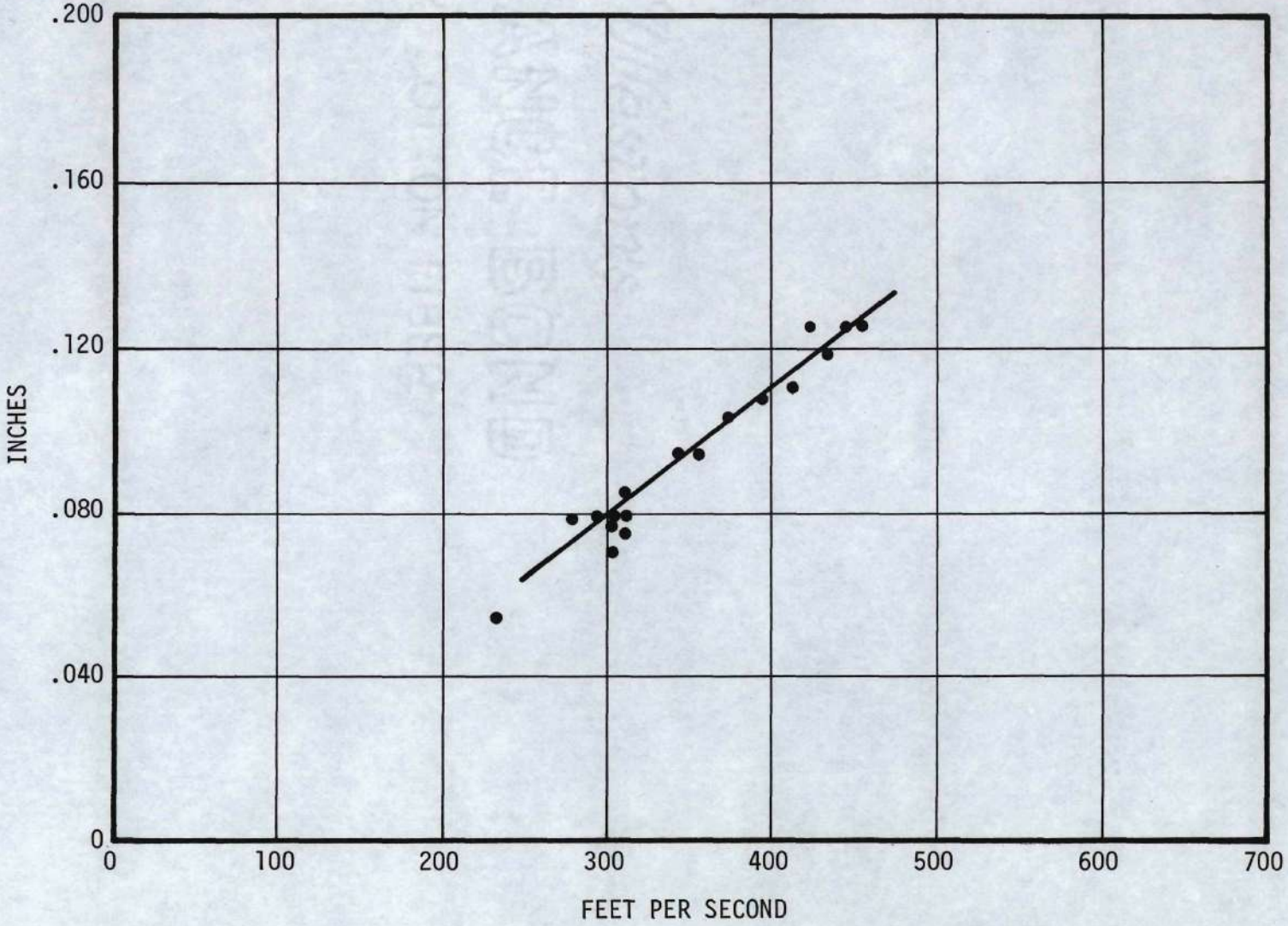

Figure 13. Change in Axial Length Versus Impact Velocity for S1.

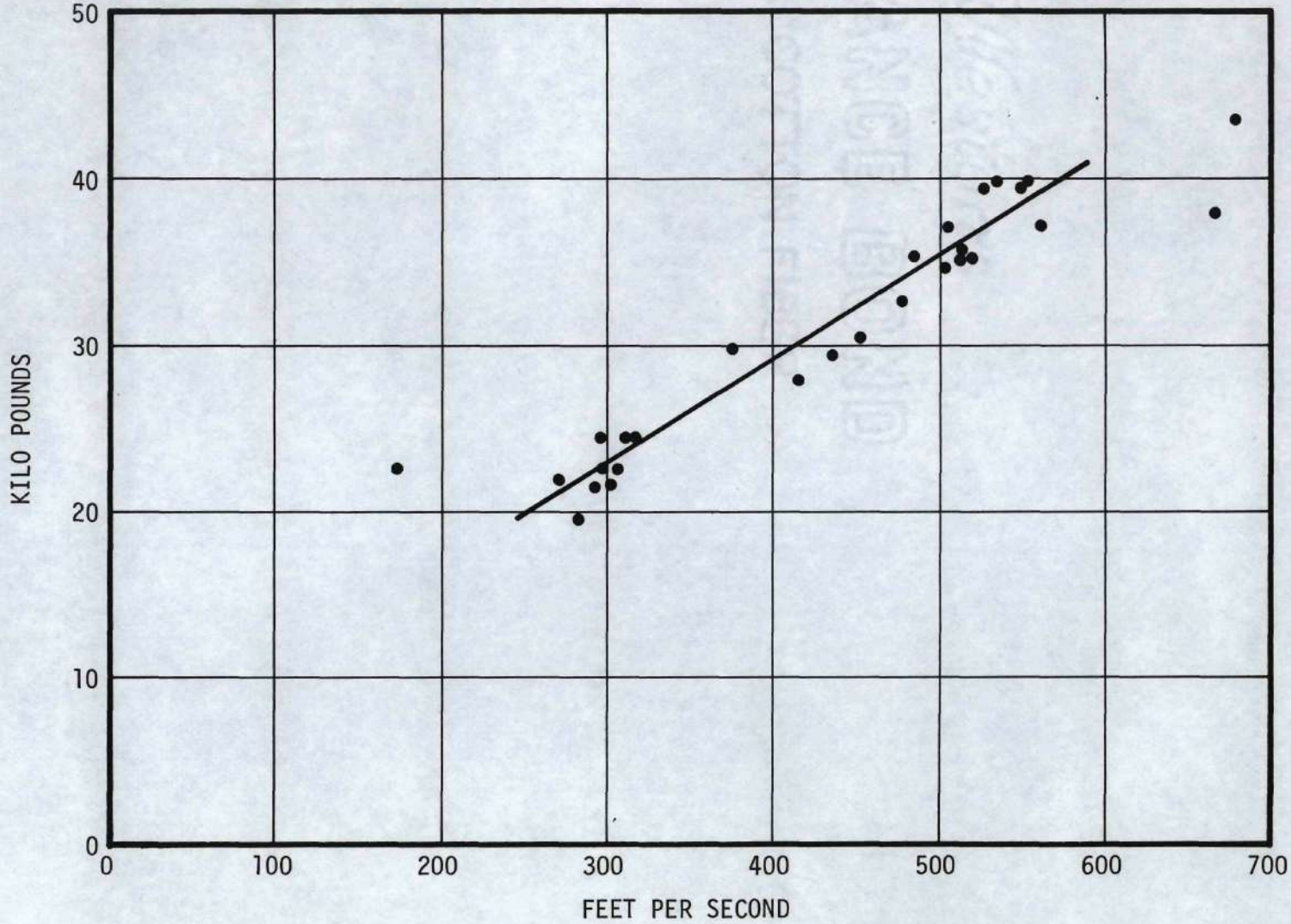

Figure 14. Peak Impact Force Versus Impact Velocity for U1.

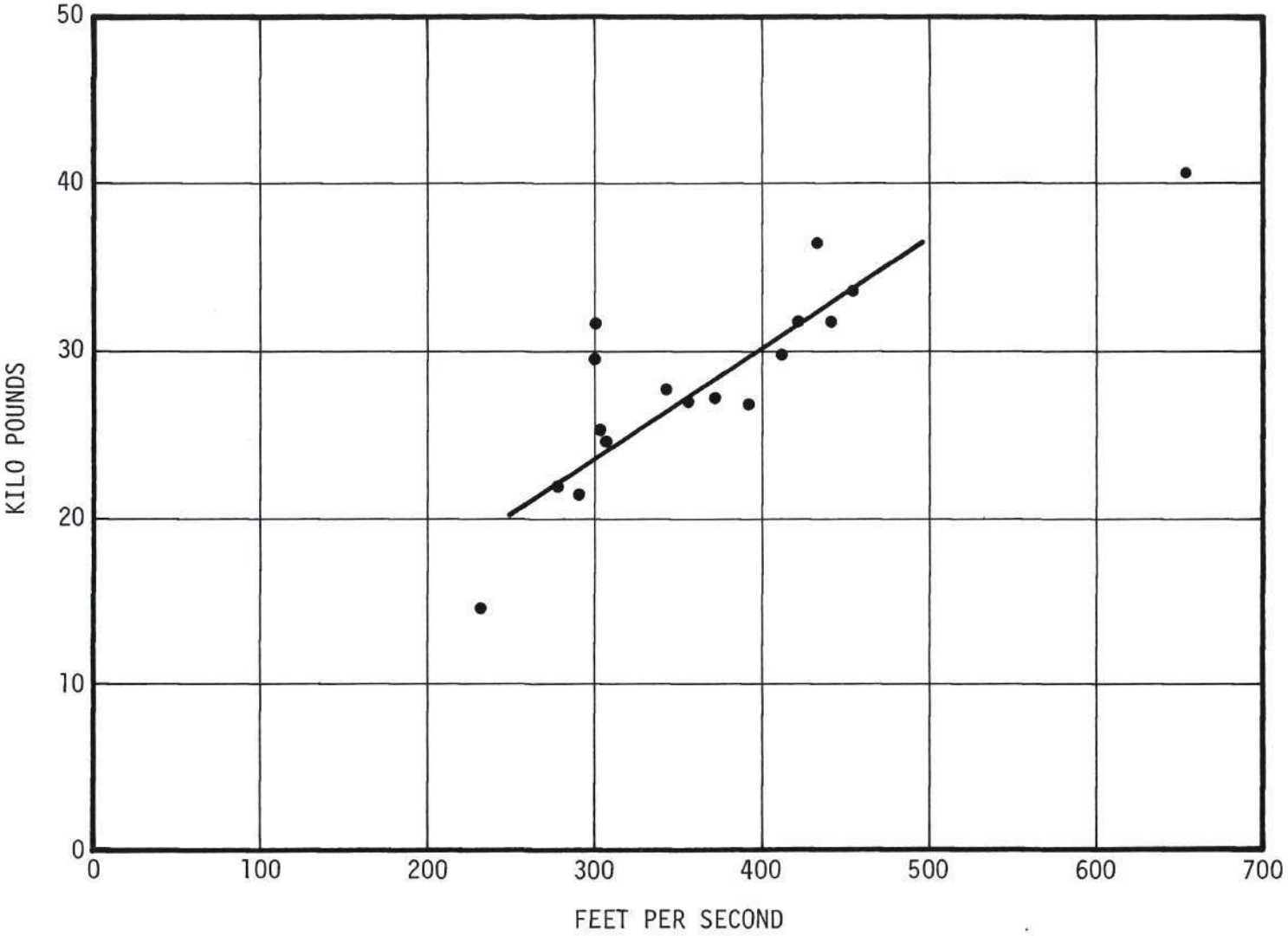

Figure 15. Peak Impact Force Versus Impact Velocity for S1.

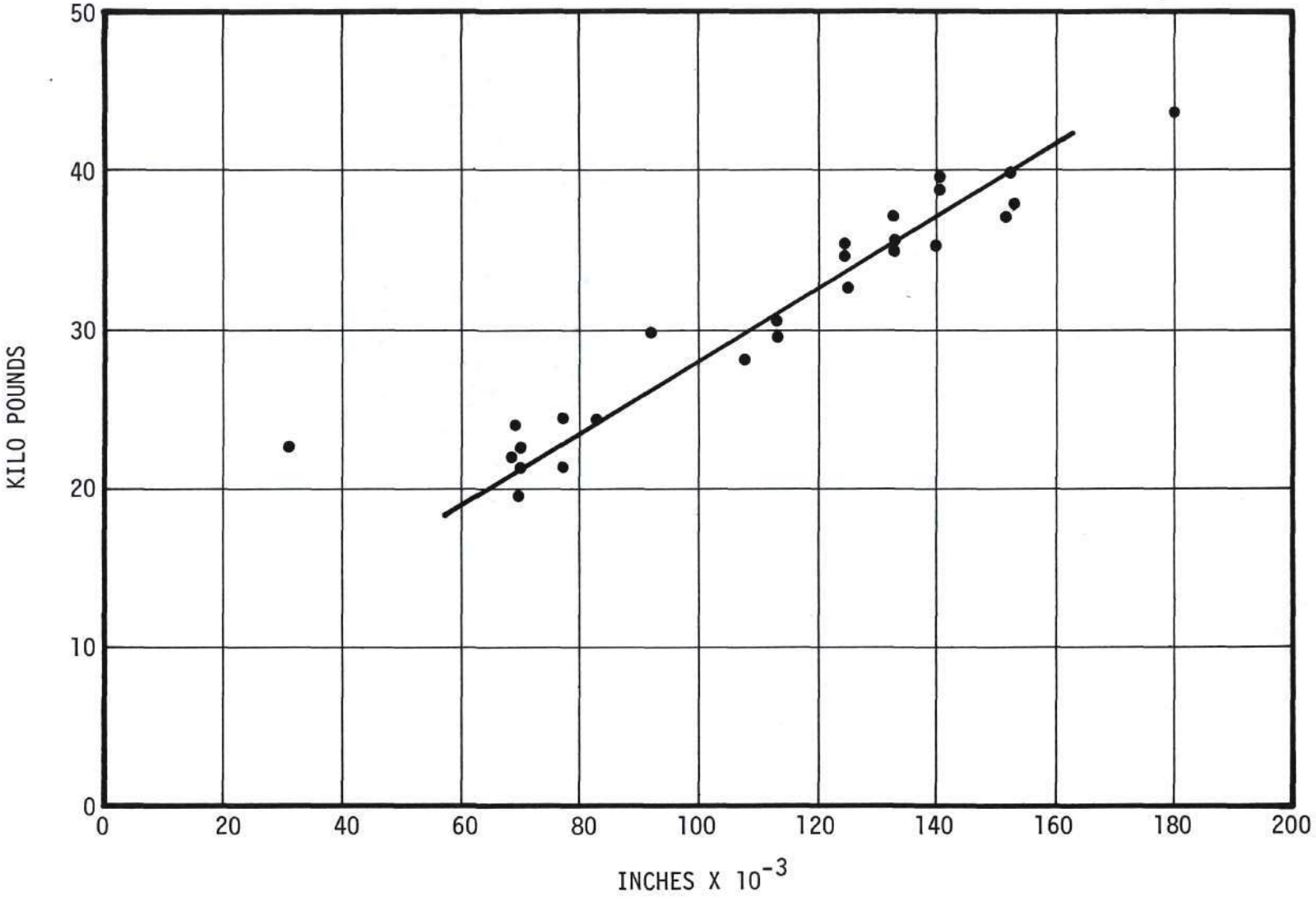

Figure 16. Peak Impact Force Versus Change in Axial Length for U1.

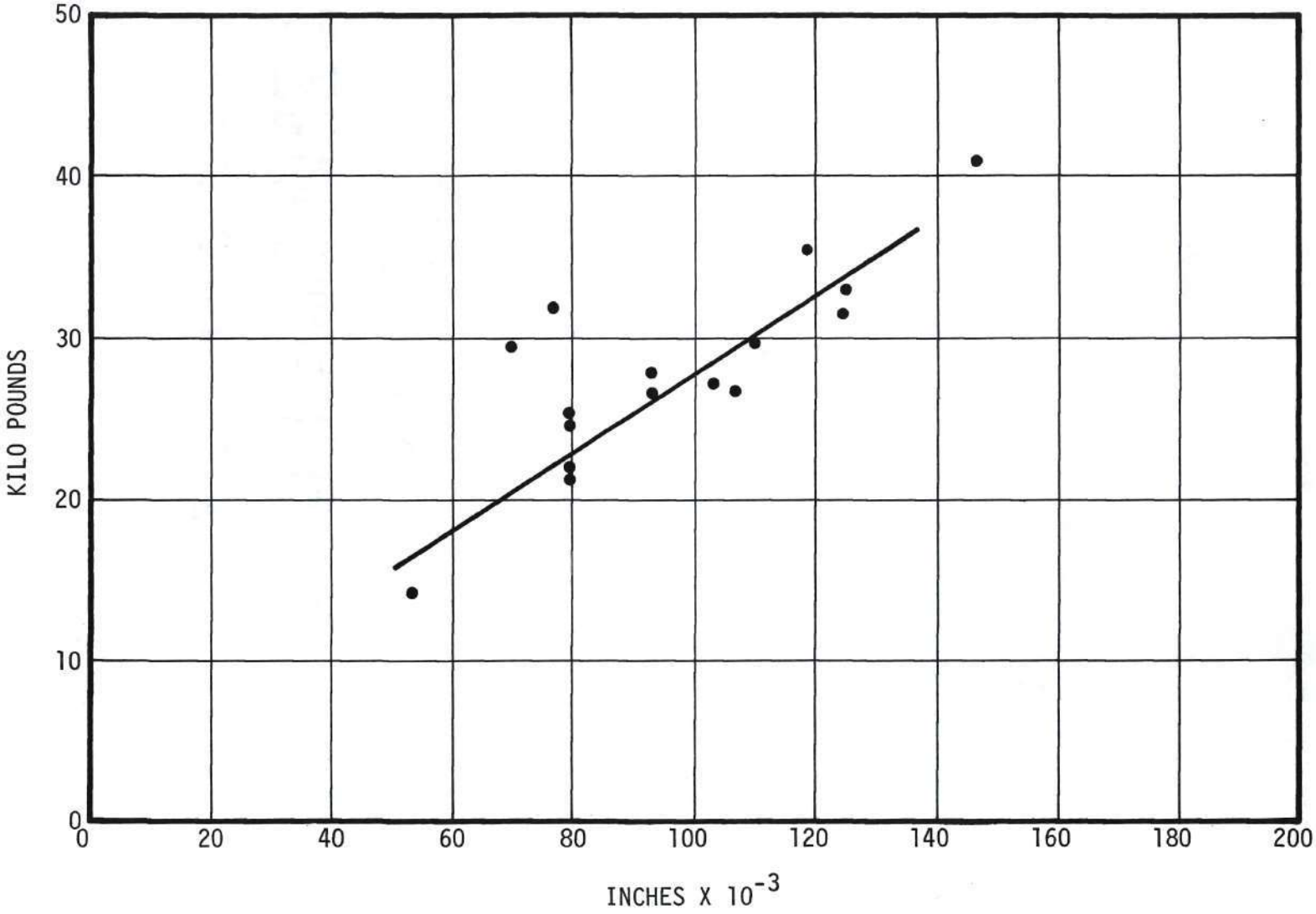

Figure 17. Peak Impact Force Versus Change in Axial Length for S1.

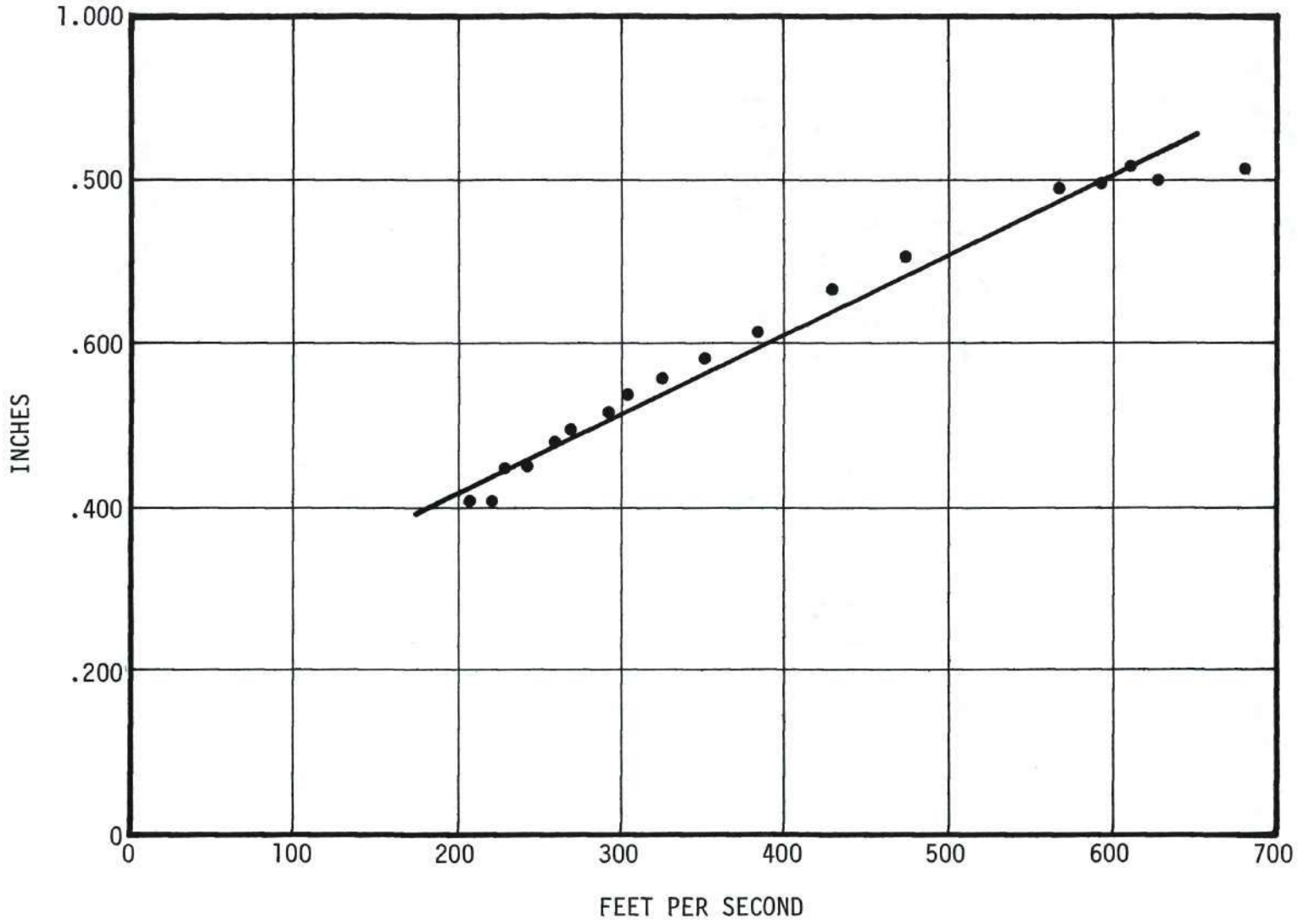

Figure 18. Impact Area Diameter Versus Impact Velocity for U2.

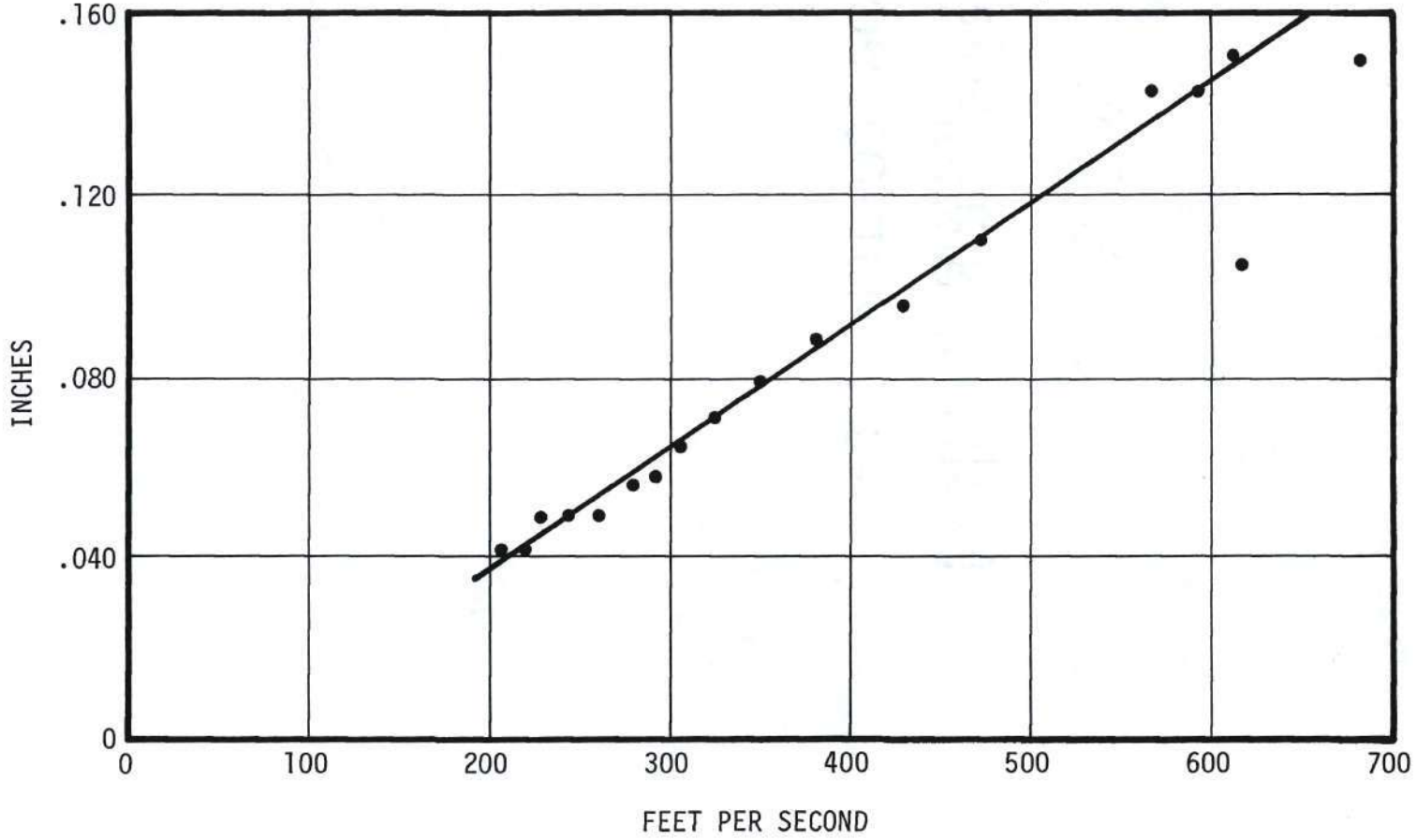

Figure 19. Change in Axial Length Versus Impact Velocity for U2.

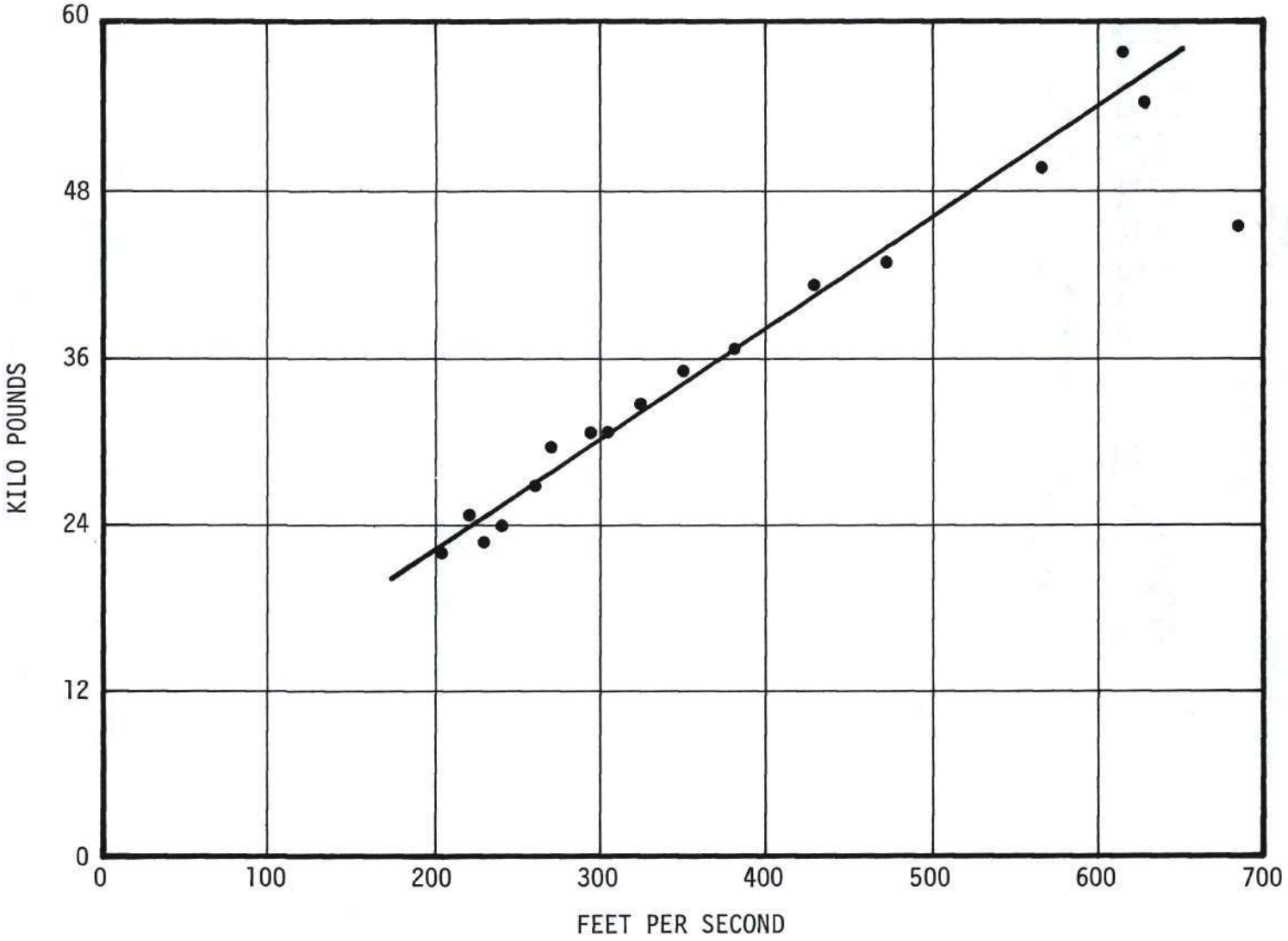

Figure 20. Peak Impact Force Versus Impact Velocity for U2.

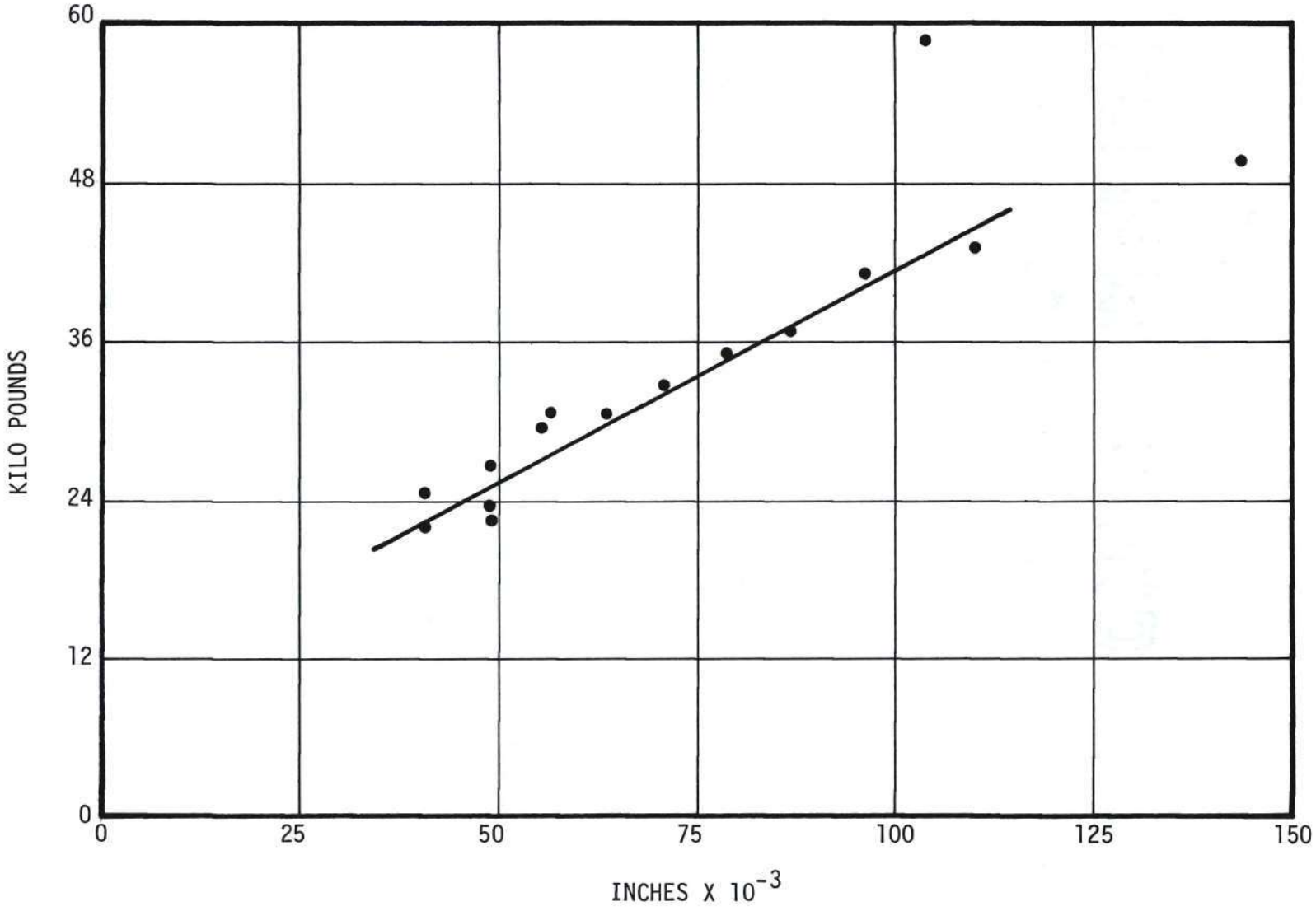

Figure 21. Peak Impact Force Versus Change in Axial Length for U2.

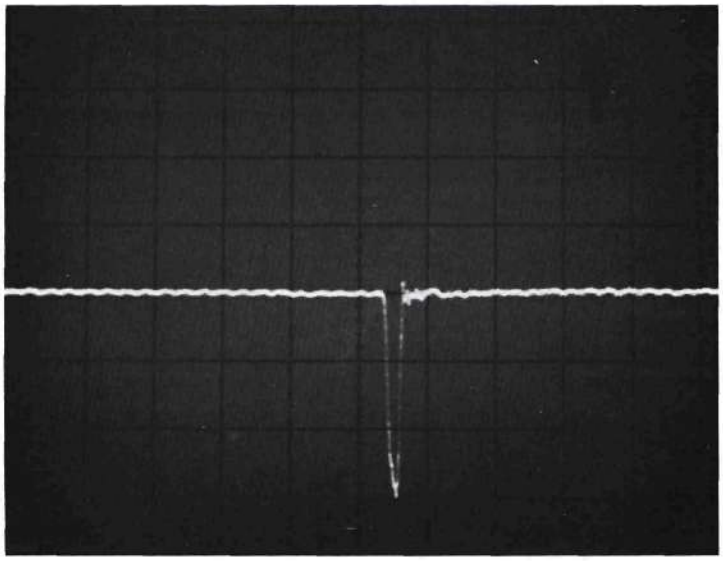

Impact Velocity	538 fps
Sweep Rate	0.2 msec. per cm.
Sensitivity	1.0 mvolt per cm.

Figure 22. A Typical Strain Gage Pulse.

BIBLIOGRAPHY

1. Stoneking, C. E., "A Study of Impact Effects on Spherical Shells, Quarterly Progress Reports #1-10," Georgia Institute of Technology, Engineering Experiment Station, 1964-1966.

2. Young, C. W., C. E. Stoneking, and J. L. Colp, "Containment Capsule Impact Safety Study, Phase A, Progress Report," Sandia Corporation, SC-RR-65-9.

3. Turnbow, J. W., "Stress-Strain Characteristics of Materials at High Strain Rates," Part III. The University of Texas, Structural Mechanics Research Laboratory, Contract AT(29-2)-621. Jan. 1959.

4. Davies, R. M., "A Critical Study of the Hopkinson Pressure Bar," Philosophic Transactions of the Royal Society 240 Sec. A, 375-457, 1948.